A novel imaging-compatible sciatic nerve schwannoma model

Okay Saydam[a],[*],[+], **Gokhan Baris Ozdener**, **Ozlem Senol**[a], **Arda Mizrak**[a], **Shilpa Prabhakar**[a], **Anat O. Stemmer-Rachamimov**[b], **Xandra O. Breakefield**[a], and **Gary J. Brenner**[c],[*]

[a]Departments of Neurology and Radiology, Massachusetts General Hospital, and Neuroscience Program, Harvard Medical School, Boston, Massachusetts, 02129 USA

[b]Molecular Neuro-oncology Laboratory and Department of Pathology, Massachusetts General Hospital, Harvard Medical School, Boston, Massachusetts, 02129 USA

[c]Department of Anesthesia and Critical Care, Massachusetts General Hospital, Harvard Medical School, Boston, MA

Abstract

Benign schwannomas are common tumors of the cranial and peripheral nerves, causing pain and loss of function. The development of effective therapy for these tumors has been hampered by the lack of relevant experimental *in vivo* models for convenient testing. Here, we describe a novel schwannoma model in which an immortalized human schwannoma cell line, HEI-193, established from an neurofibromatosis type 2 patient, has been stably transduced with fluorescent protein and luciferase reporters and implanted within the sciatic nerve of nude mice. These cells reliably formed a tumor within several weeks which had pathologic characteristics of schwannoma tumors. This model system will be useful for investigation of schwannoma biology and for preclinical assessment of therapeutic agents.

Keywords

schwannoma; NF2; sciatic nerve tumor model

1. Introduction

Schwannomas arise from Schwann cells, the myleninating cell of the peripheral nervous system (MacCollin et al., 2005). Schwannomas typically result from loss of the neurofibromatosis 2 (NF2) tumor suppressor gene (Martuza and Eldridge, 1988), but can also arise through other genetic mechanisms such as inactivating mutations in *PRKAR1A* (Jones et al., 2008) or loss of heterozygosity (LOH) of SMARCB1 (Boyd et al., 2008) genes. Current therapy for schwannomas involves surgery followed by radiotherapy or

[*]Corresponding authors: Gary J. Brenner, M.D., Ph.D., Department of Anesthesia and Critical Care, Massachusetts General Hospital, CNY 149, Room 4309, Building 149, 13th Street, Charlestown, MA 02129, Phone: 617-726-8810, Fax: 617-724-3632, GJBRENNER@PARTNERS.ORG. Okay Saydam, Ph.D, Departments of Neurology and Radiology, Massachusetts General Hospital/ Harvard Medical School, Building 149, 13th Street, 6th Floor, Room: 6101, Charlestown, MA 02129, Phone: 617-726-5730, Fax: 617-724-1537, osaydam@partners.org.
[+]Okay Saydam, Ph.D, Current address: Department of Pediatrics, Medical University of Vienna, 1090 Austria, okay.saydam@meduniwien.ac.at

chemotherapy. Surgical resection of nerve-sheath tumors is difficult due to possible damage to critical nerves or other structures, such as blood vessels. Therefore, there is a need for the development of new, less invasive therapeutic strategies for the treatment of these tumors. One major limitation to the development of new treatment modalities is the lack of an appropriate and convenient tumor model. Although several mouse NF2-schwannoma models have been generated, their use is limited due to (i) random location or the long time interval required for tumor formation (Giovannini et al., 1999 and 2000) and (ii) the difficulty in assessing changes in tumor size over time in individual animals (Messerli et al., 2006). Therefore, in the present study, we describe a novel schwannoma tumor model that was generated via implantation of an immortalized human schwannoma cell line derived from an NF2 patient directly into the sciatic nerve. Stable transduction of these cells with expression cassettes for firefly luciferase (Fluc) (Badr et al., 2007) and the fluorescent protein, mCherry (Jones et al., 2008), allowed monitoring of tumor growth and pathology, respectively. In vivo bioluminescent imaging was used to non-invasively monitor the longitudinal growth of tumors, and post-mortum sciatic nerve histology was used to further characterize interneuronal localization and morphology of the implanted malignant cells.

2. Results

In order to develop a relevant tumor model for schwannomas, we employed the HEI-193 cell line, an immortalized human schwannoma line previously established from tumor cells from an NF2 patient (Hung et al., 2002). We stably transduced these cells by infection with a lentivirus vector encoding expression cassettes for Fluc and mCherry in order to monitor tumor growth *in vivo* by bioluminescence imaging, as described previously (Saydam et al., 2009). Infectability of this cell line was 99% as determined by mCherry expression under fluorescence microscopy (data not shown). These cells were implanted directly into two major branches, tibial and common peroneal, of the left sciatic nerve of nude mice (1 µl of injected total – 0.5 µl per nerve). Subsequent tumor growth was monitored at five to seven day intervals by *in vivo* bioluminescence imaging over 10 weeks. Three independent experiments (N=5 mice per experiment) were performed using different numbers of implanted tumor cells: they were 3×10^4, 10^5, 3×10^5. As shown in Figure 1A (with quantification shown in Figure 2), we observed a gradual increase in tumor volume over 10 weeks after tumor implantation in 13 of these 15 mice, with a consistent logarithmic rate in average $8 \times 10^3 \pm 2.1 \times 10^3$, $9.3 \times 10^3 \pm 1.27 \times 10^3$, and $10^4 \pm 3.6 \times 10^3$ photons/minute/day of tumor growth in 30,000, 100,000, and 300,00 cell groups, respectively. As shown in figure 2, there is an initial linear growth phase followed by exponential growth; this occurred independent of the number of cells implanted. Once tumors were established and exponential growth began, the doubling times were quite similar between the 3 groups (18, 16 and 24 days in 30,000, 100,000 and 300,000 groups, respectively). There is proportional growth when comparing 30,000 and 100,000 implanted cells, but not between 100,000 and 300,000. We believe that this is because the ability of the sciatic nerve to support tumor growth becomes saturated with the largest number of cells (300,000), and may be due to limitations in the ability of nerve to provide growth supportive factors or physical constraints since the tumor grows entirely within the parenchyma of the nerve.

These data show the high reproducibility of this tumor model, which provides a measurable rate of tumor growth over a 10 week period. Bioluminescence images of groups are shown in Figure 1A. Ten weeks after implantation animals were euthanized and tumor-containing sciatic nerves were photographed for comparison to control nerve, i.e., contralateral (right) nerves of tumor-implanted mice. There were no apparent gross neurologic deficits in hind-limb on the side of the tumor-implanted sciatic nerve. The size of the tumor-bearing nerve was enlarged (Fig. 1B, right) compared to control (Fig. 1B, middle). Furthermore, in fluorescent histochemical analysis of sections from the same tumor samples, tumor cells

were found to express mCherry (Fig. 1C). These tumors were partially positive for the schwannoma cell marker, S100, by immunocytochemical staining of the same tumor samples (Fig. 1C). Hematoxylin and eosin sections showed that tumor cells have large oval, hyperchromatic nuclei and scant cytoplasm. The tumor is infiltrating the nerve, dissecting between individual nerve fibers; similar to the pattern of growth seen in human peripheral nerve sheath tumors (Fig. 1D). Quantification of bioluminescent signal in Figure 1A is shown in Figure 2. As the growth curves demonstrate, this approach provides a schwannoma model which grows at a reproducible and relatively slow rate in a biologically relevant location (i.e., within a peripheral nerve) and can be non-invasively monitored by bioluminescence and fluorescent reporter proteins.

3. Methods

Human schwannoma cell line HEI-193 was established from a benign schwannoma tumor from an NF2 patient immortalized with retroviral mediated HPV E6-E7 gene expression and obtained from the House Ear Institute (Hung et al., 2002). These cell lines have been transduced with lentivirus expressing Fluc and mCherry genes as described previously (Saydam et al., 2009) and were cultured as described previously (Hung et al., 2002).

3.1 Tumor implantation and bioluminescence imaging

HEI-193 cells were trypsinized, rinsed, and implanted in 1 µl culture medium into the sciatic nerve of athymic mice (nu/nu, 5-week-old females; Cox 7 breeding facility, MGH). *In vivo* bioluminescence imaging was performed, as described previously (Saydam et al., 2009).

3.2 HC staining

Immunohistochemistry with immunofluorescent staining was conducted, as previously described (Brenner et al., 2004). mCherry was visualized directly. S100 (1:400, Dako, Glostrun Denman, Carpinteria, CA) was visualized using fluorescent immunohistochemistry. Images were acquired using a Nikon Eclipse E800 microscope.

4. Discussion

This study provides the first report of a schwannoma tumor model grown in the sciatic nerve, an environment that is biologically relevant for this neoplasm. In this model, we showed reproducible tumor development (13 out of 15 mice) and a constant, measurable rate of tumor growth 1–4 weeks after implantation. The use of reporter proteins provided a non-invasive and reliable means to monitor growth *in vivo* by bioluminescence and to locate tumor cells in the sciatic nerve by fluorescence microscopy. Although recent mouse models of NF2 uncovered several unknown key points concerning the molecular pathogenesis of schwannomas (Giovannini et al., 1999 and 2000; Messerli et al., 2006), their use as a model system to investigate and/or develop novel therapeutic strategies has been limited due to random location along nerve fibers and/or slow tumor growth (Giovannini et al., 1999 and 2000; Messerli et al., 2006). In the present study, we provided a novel sciatic tumor model for schwannomas and this model offers a reproducible tumor development in a short time period after tumor implantation between 2–3 weeks. The model has significant advantages over existing schwannoma models in that the tumors are in a known location and grow at consistent growth rate over 2 months. Further, by stably transducing these cells with an expression cassette for Fluc we are able to non-invasively quantify the growth/regression of these tumors using longitudinal *in vivo* bioluminescence imaging. Moreover, this model represents a new preclinical model that will allow testing of a variety of biological modifiers on tumor growth in an environment that is biologically relevant.

4.1 Conclusion

In conclusion, in this study we describe a novel sciatic nerve tumor model for schwannoma. This model system will be useful for investigation of schwannoma biology and for preclinical assessment of therapeutic agents.

Abbreviations

NF2	neurofibromatosis 2
Fluc	firefly luciferase
LOH	loss of heterozygosity

Acknowledgments

References

Badr CE, Hewett JW, Breakefield XO, Tannous BA. A highly sensitive assay for monitoring the secretory pathway and ER stress. PLoS ONE. 2007; 2:e571. [PubMed: 17593970]

Boyd C, Smith MJ, Kluwe L, Balogh A, Maccollin M, Plotkin SR. Alterations in the SMARCB1 (INI1) tumor suppressor gene in familial schwannomatosis. Clin Genet. 2008; 74:358–366. [PubMed: 18647326]

Brenner GJ, Ji RR, Shaffer S, Woolf CJ. Peripheral noxious stimulation induces phosphorylation of the NMDA receptor NR1 subunit at the PKC-dependent site, serine-896, in spinal cord dorsal horn neurons. Eur J Neurosci. 2004; 20:375–384. [PubMed: 15233747]

Giovannini M, Robanus-Maandag E, Niwa-Kawakita M, van der Valk M, Woodruff JM, Goutebroze L, Mérel P, Berns A, Thomas G. Schwann cell hyperplasia and tumors in transgenic mice expressing a naturally occurring mutant NF2 protein. Genes Dev. 1999; 13:978–986. [PubMed: 10215625]

Giovannini M, Robanus-Maandag E, van der Valk M, Niwa-Kawakita M, Abramowski V, Goutebroze L, Woodruff JM, Berns A, Thomas G. Conditional biallelic Nf2 mutation in the mouse promotes manifestations of human neurofibromatosis type 2. Genes Dev. 2000; 14:1617–1630. [PubMed: 10887156]

Hung G, Li X, Faudoa R, Xeu Z, Kluwe L, Rhim JS, Slattery W, Lim D. Establishment and characterization of a schwannoma cell line from a patient with neurofibromatosis 2. Int J Oncol. 2002; 20:475–482. [PubMed: 11836557]

Jones GN, Tep C, Towns WHn, Mihai G, Tonks ID, Kay GF, Schmalbrock PM, Stemmer-Rachamimov AO, Yoon SO, Kirschner LS. Tissue-specific ablation of Prkar1a causes schwannomas by suppressing neurofibromatosis protein production. Neoplasia. 2008; 10:1213–1221. [PubMed: 18953430]

MacCollin M, Chiocca EA, Evans DG, Friedman JM, Horvitz R, Jaramillo D, Lev M, Mautner VF, Niimura M, Plotkin SR, Sang CN, Stemmer-Rachamimov A, Roach ES. Diagnostic criteria for schwannomatosis. Neurology. 2005; 64:1838–1845. [PubMed: 15955931]

Martuza RL, Eldridge R. Neurofibromatosis 2 (bilateral acoustic neurofibromatosis). N Engl J Med. 1988; 318:684–688. [PubMed: 3125435]

Messerli SM, Prabhakar S, Tang Y, Mahmood U, Weissleder R, Bronson R, Martuza R, Rabkin S, Breakefield XO. Treatment of schwannomas with an oncolytic HSV recombinant virus in murine models of neurofibromatosis type 2. Hum Gene Ther. 2006; 17:20–30. [PubMed: 16409122]

Saydam O, Shen Y, Würdinger T, Senol O, Boke E, James MF, Tannous BA, Stemmer-Rachamimov AO, Yi M, Stephens RM, Fraefel C, Gusella JF, Krichevsky AM, Breakefield XO. Downregulated microRNA-200a in meningiomas promotes tumor growth by reducing E-cadherin and activating

the Wnt/{beta}-catenin signaling pathway. Mol Cell Biol. 2009; 29:5923–5940. [PubMed: 19703993]
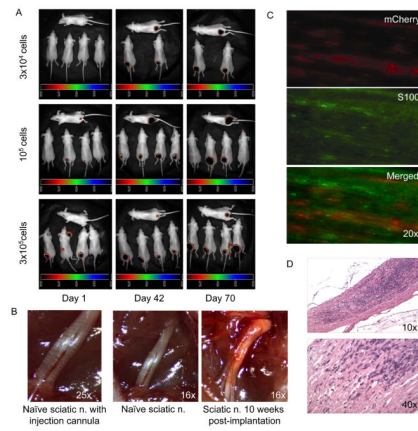
Figure 1. Sciatic nerve schwannoma model

(A) Human schwannoma cells (HEI-193) stably expressing Fluc and mCherry were injected (in 1 µl of culturing medium) into the sciatic nerve of nude mice. In vivo tumor progression was monitored weekly using bioluminescence for 70 days. Bioluminescent images from 15 mice are shown with a pseudocolor bar to indicate degree of bioluminescence. (B) The HEI-193 cells were injected using a glass micropitette (left panel showing pipette next to an un-injected sciatic nerve for size comparison); sciatic nerves containing HEI-193-FC-derived tumors were imaged in vivo 2 months after HEI-193-FC implantation (right panel demonstrating altered gross morphology of sciatic nerve; left panal showing naïve sciatic nerve for comparison); images were acquired through a dissecting stereo-microscope. Tumor-impanted nerves were then removed for histologic analysis. (C) Sections were stained for S100 (FITC) and fluorescent microscopy performed to assess co-localization with mCherry. (D). Hematoxylin and eosin staining of longitudinal sections of the sciatic nerve post-implantation of HEI-193.
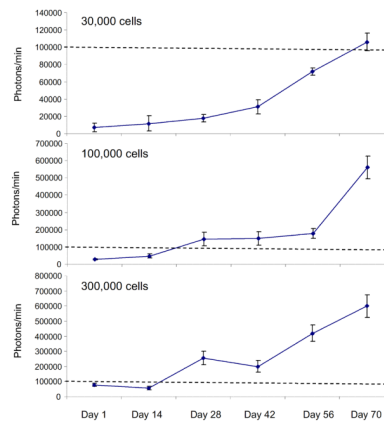
Figure 2. Quantification of bioluminescent signals
Tumor growth in Figure 1A was monitored by *in vivo* bioluminescence imaging using a CCD camera and RSI IDL 6.3 program was used for the quantification of photo counts. Relative luciferase activity is shown as the mean photons/minute ± S.D. Dashed lines indicate 100,000 photons/minute (note: ordinate scale differs in 3 panels).